

# Photochemical generation, intramolecular reactions, and spectroscopic detection of oxonium ylide and carbene intermediates in a crystalline *ortho*-(1,3-dioxolan-2-yl)-diaryldiazomethane†‡

Miguel A. Garcia-Garibay\* and Hung Dang

Received 19th August 2008, Accepted 5th December 2008

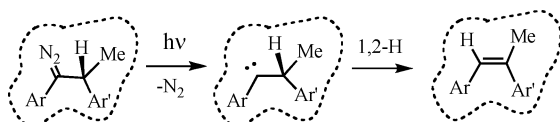
First published as an Advance Article on the web 3rd February 2009

DOI: 10.1039/b814387k

Photochemical excitation of a diaryldiazomethane with an *ortho*-acetal both in solution and in crystals led to products that originate from the expected diarylcarbene and form an intramolecular oxonium ylide. While crystals strongly favored the formation of a benzocyclobutane by intramolecular hydrogen abstraction in the triplet carbene, reactions in benzene led exclusively to products that derive from the oxonium ylide. Studies in methyl cyclohexane glasses and in mixed crystals at 77 K led to the spectroscopic detection of triplet carbene  $^3\text{C}$ , which partially transformed into a new species that we assign as the sought-after oxonium ylide **Y**. The formation of a formally ionic intermediate suggests that the scope of reactions by reactive intermediates in crystalline solids may be broader than it is generally assumed.

## Introduction

Although reactive intermediates tend to follow numerous reaction pathways in solution,<sup>1</sup> our group has shown that radical pairs<sup>2</sup> and carbenes<sup>3,4</sup> react with remarkable selectivities and specificities when generated in crystals of their precursors.<sup>5</sup> We previously reported that ruby-red crystals of 1,2-diaryldiazopropanes transform into (*Z*)-1,2-diarylpropenes in nearly quantitative yields by a highly selective 1,2-H shift of their photochemically generated carbene intermediates (Scheme 1).<sup>6,7</sup> Reactions in solution yielded a mixture of products that included 1,2-H shifts, 1,2-Ar migrations and reactions with solvents.<sup>8</sup> Recognizing that crystalline solids may control the reactivity of high-energy species while providing valuable structural insight from X-ray diffraction data,<sup>9</sup> we decided to explore the generation and reactivity of oxonium ylides<sup>10</sup> (**Y**, Scheme 2). Our interest in oxonium ylides stems from their potential for the synthesis of complex structures<sup>11</sup> and, more importantly, from the possibility of increasing the number of reactions in crystalline solids.

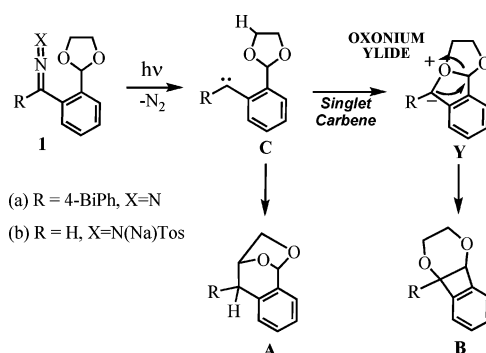


**Scheme 1** Selective 1,2-H shift in 1,2-diarylpropylidenes generated in crystals of their diazo precursors.

Department of Chemistry and Biochemistry, University of California, 405 Hilgard Ave, Los Angeles, CA, USA. E-mail: mgg@chem.ucla.edu; Fax: +1 310 825 0767; Tel: +1 310 825 3159

† Electronic supplementary information (ESI) available:  $^1\text{H}$  and  $^{13}\text{C}$  NMR spectra of compounds **1a**, **6**, **8**, **9** and **10**. Additional details of the crystal structures determinations of **1a** and **8**. CCDC reference numbers 698857–698858. For ESI and crystallographic data in CIF or other electronic format see DOI: 10.1039/b814387k

‡ This work was supported by NSF grants CHE0551938 and DMR0605688

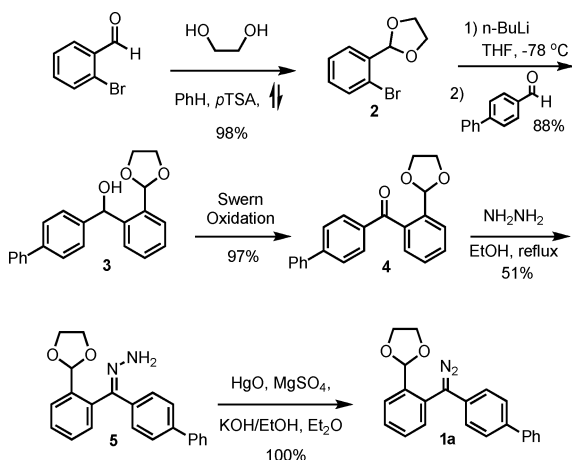


**Scheme 2** Formation of an oxonium ylide from an aryl carbene with an *ortho*-dioxolane.

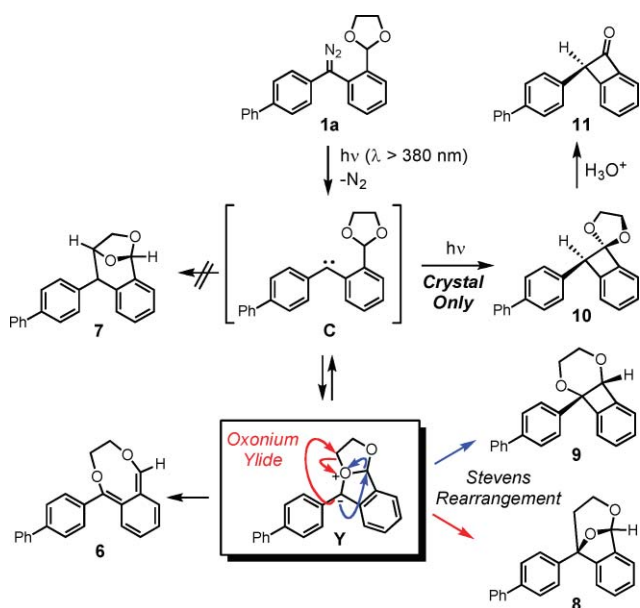
We selected for this study samples of *ortho*-(1,3-dioxolan-2-yl)-diaryldiazomethane derivative **1a** (Scheme 2, R = 4-biphenyl, X = N). Compound **1a** is a crystalline and high-melting analog of the monoaryldiazomethane derived from the sodium salt of tosyl hydrazone **1b** (R = H, X = N(Na)Ts) previously studied in solution by Kirmse and Kund.<sup>12</sup> As illustrated in Scheme 2, oxonium ylide **Y** can be ideally described as a ground state species with a positively charged hypervalent oxygen linked directly to a carbon atom carrying an unshared pair of electrons. The oxonium ylide is formed by donation of a lone pair from the adjacent oxygen to the empty p-orbital of the  $\text{sp}^2$ -hybridized singlet state carbene ( $^1\text{C}$ ), which in the case of diaryl carbenes exists in small equilibrium concentrations as compared to the more stable triplet ( $^3\text{C}$ ).<sup>13</sup> Recent studies by Moss *et al.* have confirmed that the formation of oxonium ylides depends strongly on the nature of the carbene and the ether. While it is calculated that favorable cases give rise to typical C–O sigma bonds, others are best described in terms of a weak solvation effect.<sup>14</sup> The intermediacy of an oxonium ylide in the case of sodium tosyl hydrazone **1b** can be deduced from product analysis. UV irradiation in a non-reactive solvent primarily produced 6,8-dioxabicyclo[3.2.1]octane **A** (10%)

and 1,4-dioxane **B** (66%).<sup>12</sup> It was suggested that **A** forms by formal insertion of the carbene into a C–H bond of the neighboring dioxolane while formation of **B** was assigned to a formal 1,2-alkyl migration (Stevens-like rearrangement) of ylide **Y**.<sup>12</sup>

Expecting distinguishable products from the carbene and the ylide, we selected compound **1a** as the starting point to analyze the formation of the latter. In this paper we wish to report the synthesis and X-ray structure of diaryldiazo acetal **1a** (Scheme 3), its solution and solid state photochemistry, as well as spectroscopic evidence for the detection of both the carbene and oxonium ylide. As reported below, the solution photochemistry of diazo **1a** in benzene at ambient temperature differs from that of the diazo derived from the tosyl hydrazone salt **1b** in diglyme. Irradiation of **1a** resulted in three major products that we assign as originating from the oxonium ylide (Scheme 4). Two of these products (**8** and **9**) can be accounted for by 1,2-alkyl migrations (Stevens rearrangements) and the third one (**6**) by an electrocyclic ring



**Scheme 3** Synthesis of diaryldiazomethane **1a**.



**Scheme 4** Formation of carbene (**C**) and ylide (**Y**) intermediates and their more likely intramolecular reaction pathways.

opening. Interestingly, photochemical reactions in crystals of **1a** favor a benzocyclobutane product (**10**), which presumably derives from hydrogen-transfer and radical cyclization from the triplet carbene. Small amounts of products **8** and **9** from the oxonium ylide are also formed upon extended irradiation. Irradiation in methyl cyclohexane matrices and in mixed crystals at 77 K led to the spectroscopic detection of triplet carbene <sup>3</sup>C, which partially transformed into a new species that we assign as the sought-after oxonium ylide intermediate **Y**. Our results suggest that the ylide and the carbene exist in equilibrium in the crystal, with the triplet carbene being the dominant species.

## Results and discussion

### Synthesis and characterization of the diazo precursor

The diazo precursor **1a** was synthesized in five steps from the commercially available 2-bromobenzaldehyde (Scheme 3). Bromoacetal **2** was isolated in 98% yield after treating 2-bromobenzaldehyde with anhydrous ethylene glycol in refluxing benzene. Treatment of **2** with *n*-BuLi at  $-78\text{ }^{\circ}\text{C}$  followed by addition of 4-biphenylcarboxaldehyde gave alcohol **3** in 88% isolated yield. Swern oxidation of alcohol **3** gave ketone **4** in near quantitative yield. The next step involved refluxing ketone **4** with anhydrous hydrazine in absolute ethanol to give hydrazone **5** (51%) as a thick viscous oil that solidified after several days at room temperature. Hydrazone formation was sluggish, probably due to the steric hindrance of the ketone by the neighboring *ortho*-acetal and the biphenyl substituent. Oxidation of hydrazone **5** with mercury(II) oxide afforded diazo **1a** as deep ruby-red prisms grown from diethyl ether solutions.

The structure of diaryldiazomethane **1a** was determined by conventional spectroscopic methods and confirmed by single crystal X-ray diffraction analysis. Solution NMR carried out in deuterated chloroform showed the <sup>1</sup>H signal of the acetal proton at 5.88 ppm and the signals of the ethylenedioxy group in the range of 3.93–4.13 ppm. The diazo carbon signal occurs at 122.6 ppm and the acetal carbon at 101.5 ppm.

X-Ray diffraction data acquired on deep-red prisms obtained from diethyl ether were solved in the triclinic crystal space group *P* $\bar{1}$  with one molecule in the asymmetric unit (Fig. 1). The structure of **1a** has the planes of the biphenyl and 1,3-dioxolane nearly orthogonal to that of the central *ortho*-phenylene, with the diazo moiety conjugated with the biphenyl substituent. Assuming that conformational motions will be minimal in the crystal, the feasibility of ylide formation is suggested by the relatively close distances between the prospective carbene carbon and the two

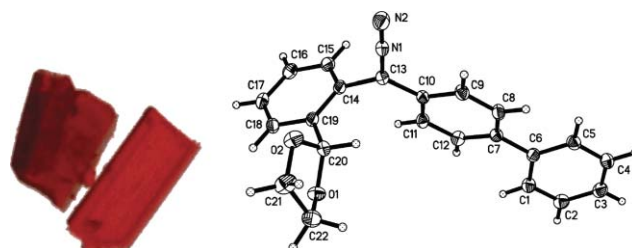


**Fig. 1** Crystals of diaryldiazomethane **1a** and ORTEP diagram with thermal ellipsoids drawn at the 50% probability level.

**Table 1** Product distribution from photolysis<sup>a</sup> of diaryldiazomethane **1a** in solution and in crystals<sup>b</sup>

Reaction medium	<b>6</b>	<b>8</b>	<b>9</b>	<b>10</b>
C <sub>6</sub> H <sub>6</sub>	15	15	43	0
Crystal	0	10	10	75

<sup>a</sup> UV irradiations were carried out with a Hanovia medium pressure Hg lamp using a  $\lambda > 290$  nm glass filter. <sup>b</sup> Isolated yields after ca. 90% of the reactant had been consumed.

acetal oxygens with O1–C13 and O2–C13 distances of 3.85 Å and 4.10 Å, respectively.

### Photochemical experiments and product analyses in solution

Photochemical experiments were carried out with argon-exchanged 0.1 M benzene solutions at ambient temperature filtering the output of a 400 W mercury vapor Hanovia lamp with a  $\lambda > 380$  nm cutoff filter (Table 1). Analysis of the reaction mixture by thin layer chromatography and <sup>1</sup>H NMR revealed three major products, which were subsequently separated on silica gel using a 3 : 1 v/v mixture of methylene chloride and hexane. The three compounds were isolated in ca. 43%, 15% and 15% yields, and were later assigned the structures **9**, **6** and **8** (Scheme 3), respectively. Although the NMR spectra of compound **8** originally suggested that it might correspond to structure **7**, as expected from the report of compound **1b**, the correct structure was determined by single crystal X-ray diffraction. As described in more detail below, reactions in crystals produced benzocyclobutane **10** as the major product along with small amounts of **8** and **9**.

Samples of *o*-QDM **6** were characterized by their pale yellow color and a UV spectrum with a  $\lambda_{\text{max}} = 372$  nm that extends up to ca. 475 nm, which is characteristic of simple *ortho*-quinodimethanes (Fig. 2).<sup>15</sup> Key to the assignment is the fact that there are only two carbon signals in the sp<sup>3</sup> region at 66.22 and 39.08 ppm, respectively, which are assigned to the ethylenedioxy bridge. The structure was also identified by the distribution of

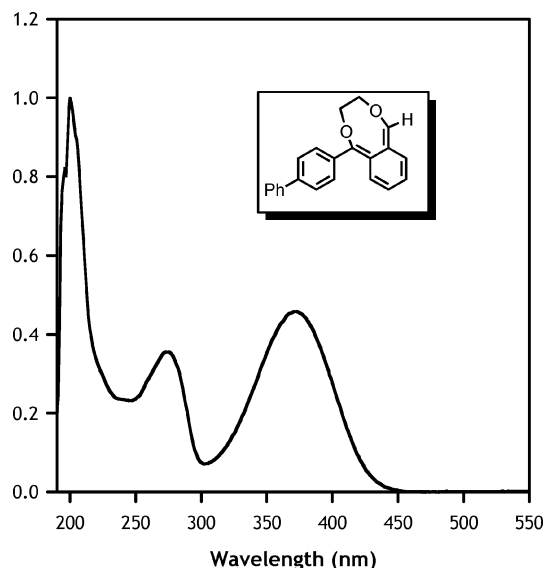
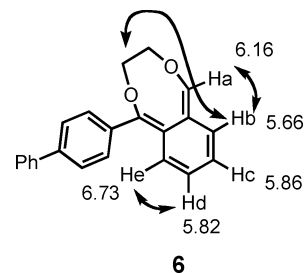


**Fig. 2** UV-Vis spectrum of *o*-QDM **6** in methyl cyclohexane.

aromatic, vinylic and ethylenedioxy hydrogens in the <sup>1</sup>H NMR spectrum, which were assigned with the help of <sup>1</sup>H–<sup>1</sup>H COSY and <sup>1</sup>H–<sup>1</sup>H NOESY measurements. Three sets of aromatic signals at 7.80 ppm (2H), 7.43 ppm (4H) and 7.20 ppm (3H) ppm show the expected cross-correlations and account for the nine hydrogens of the biphenyl group. A spin system corresponding to the four vinylic hydrogens of the *ortho*-quinodimethane ring (Hb–He) occurs between 6.73 and 5.66 ppm (Scheme 5). The isolated enol ether hydrogen (Ha) appears as a singlet at 6.16 ppm. Signals corresponding to the ethylenedioxy bridge occur as multiplets centered at 3.77, 3.69, 2.07 and 1.44 ppm, with chemical shifts that suggest shielding effects from the neighboring  $\pi$ -systems. The <sup>1</sup>H–<sup>1</sup>H NOESY spectrum shows cross peaks between Ha and Hb, which helps identify the resonances corresponding to Hc–He. A cross peak between Hb and the most shielded signal of the ethylenedioxy group at 1.44 ppm suggests a conformation where the structure of the benzodioxacyclooctane is folded over the shielding region of the *ortho*-quinodimethane  $\pi$ -system. Samples of **6** were stable upon standing for long periods at ambient temperature showing no tendency to cyclize into benzocyclobutane **9** or towards an orbital symmetry allowed *trans*-fused analog.



**Scheme 5** Assignments and key NOE correlation to assign of *ortho*-quinodimethane **6**.

The <sup>1</sup>H spectrum of 1,4-dioxane **9** in CDCl<sub>3</sub> is characterized by a set of overlapping aromatic signals between 7.23 and 7.59 ppm (13H), a benzylic methine at 5.34 ppm and two sets of signals between 3.81–3.88 (3H) and 4.01–4.04 (1H) ppm that correspond to the ethylenedioxy bridge. The <sup>13</sup>C NMR spectrum of **9** shows the expected number of signals including 14 aromatic carbons, a quaternary cyclobutane carbon at 83.26 ppm, a cyclobutane methine at 80.38 ppm, and the two ether methylenes at 61.66 and 60.61 ppm. These signals are consistent with a 1,4-dioxane derived from a formal 1,2-shift in the oxonium intermediate. Compound **9** corresponds to the simpler analog **B** reported by Kirmse and Kund (Scheme 2).

The <sup>1</sup>H NMR spectrum of **8** in CDCl<sub>3</sub> is characterized by signals that extend from 7.65 ppm in the aromatic region all the way up to 2.07 ppm, as it might have been expected for structure **7**. However, single crystal X-ray diffraction analysis (*vide infra*) revealed the connectivity present in isomer **8**. Aromatic signals between 7.65 and 7.02 ppm account for the required 13H, a sharp singlet at 6.39 ppm is assigned to the benzylic acetal, two multiplets at 3.89 and 3.40 ppm with a <sup>2</sup>J<sub>HH</sub> = 11.8 account for a methylene attached to the oxygen atom, and two multiplets at 2.76 and 2.07 ppm with <sup>2</sup>J<sub>HH</sub> = 12.6 account for the other methylene signals. One can also detect the expected vicinal couplings. Analyses of the <sup>13</sup>C NMR and a 2D heteronuclear <sup>1</sup>H–<sup>13</sup>C HMQC spectra confirm that proton signals at 2.07 and 2.76 ppm correlate with the same carbon

at 35.70 ppm, and that signals at 3.40 and 3.89 ppm correlate with the carbon at 59.45 ppm. Likewise, the acetal proton at 6.39 ppm correlates with the carbon signal at 101.01 ppm.

The structure of **8** was corroborated by single crystal X-ray diffraction analysis (Fig. 3). Compound **8** crystallized in the monoclinic space group  $P2_1/c$ , with one molecule in the asymmetric unit and four in the unit cell ( $Z = 4$ ). The structure of **8** was confirmed as a benzobicyclo[3.2.1]octane, with the 1,3-dioxane ring adopting a chair conformation. The 4'-biphenyl substituent on C10 and the acetal proton on C3 at the bridgehead positions adopt equatorial positions on the chair of the 1,3-dioxane and the *ortho*-phenylene ring (C4–C9) occupies the axial position. The biphenyl substituent adopts a nearly planar conformation with a slight twist of the two aromatic rings (C13–C14–C17–C22 torsional angle = *ca.* 5°).

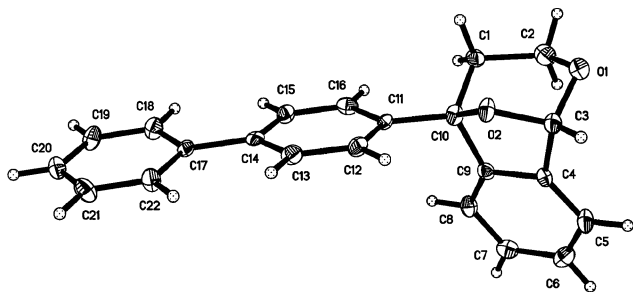
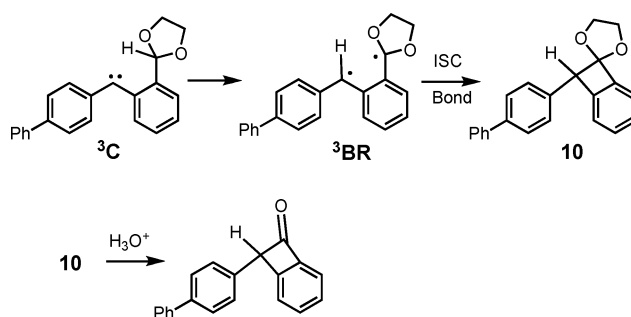


Fig. 3 ORTEP diagram of dioxabicyclo[3.2.1]octane **8** with thermal ellipsoids at the 50% probability level.

### Photochemical experiments and product analysis in the crystalline solid state

Solid-state photolysis were carried out with powdered samples of diaryldiazomethane **1a** sandwiched between microscope slides and covered with a  $\lambda > 380$  nm filter at 0 °C using a 400 W mercury vapor Hanovia lamp. While photolysis to low conversion values (*ca.* 10%) produced benzocyclobutenone acetal **10** as the only detectable product, irradiation to 95% conversion led to the formation of acetal **10** in 75% yield along with *ca.* 10% each of **8** and **9**. The spectroscopic characterization of compound **10** was based on the analysis of its spectral data and its transformation to benzocyclobutanone **11** by acid hydrolysis. A highly diagnostic benzylic cyclobutane singlet is observed at 4.97 ppm rather than close to 6.0 ppm, as it occurs when the benzylic hydrogen is part of an acetal carbon. The dioxolane ring is characterized by three multiplets at 4.19–4.11 ppm (2H), 4.03–3.99 ppm (1H) and 3.70 ppm (1H). The new quaternary ketal carbon resonates at 111.25 ppm. In a key experiment, acid hydrolysis led to the formation of the expected benzocyclobutanone, which was characterized by HRMS ( $m/z = 270.1045$  for  $C_{20}H_{14}O$ ) and by FT-IR spectroscopy, which included the characteristically high-frequency stretching band of the benzocyclobutenone C=O at  $1763\text{ cm}^{-1}$  (lit.<sup>16</sup>  $1760\text{ cm}^{-1}$ ). It is likely that compound **10** is generated from the triplet carbene ( $^3C$ ) by abstraction of the acetal hydrogen at C20 to give a triplet 1,4-biradical ( $^3BR$ ), which combines to form the four-membered ring after intersystem crossing (Scheme 6).



Scheme 6 Hydrogen abstraction by  $^3C$  leading to formation of benzocyclobutane **10**. Acid hydrolysis of the ketal in **10** leads to benzocyclobutanone **11**.

### Spectroscopic analysis of the triplet carbene and oxonium ylide in methylcyclohexane glasses and in crystals at 77 K

Since it is well known that diarylcarbenes possess a triplet ground state,<sup>1,13</sup> ylide formation must occur either immediately after denitrogenation or from a thermally equilibrated singlet. Knowing that triplet carbenes possess a relatively strong  $T_1$ – $T_0$  fluorescence,<sup>17</sup> we decided to explore the detection of the carbene and to probe the formation of the oxonium ylide (presumably from the thermally populated singlet). A dilute solution of diazo **1a** (*ca.*  $10^{-4}$  M) in spectroscopic grade methylcyclohexane (MCH) was cooled to 77 K and irradiated with  $\lambda = 340$  nm. As expected, the fluorescence excitation and emission spectra of carbene  $^3C$  are essentially identical to those of diphenyldiazomethane.<sup>16</sup> The emission spectrum consists of two maxima at 560 and 600 nm and a shoulder by 650 nm. The excitation spectrum is characterized by absorption maxima of *ca.* 350 nm, and two weaker bands corresponding to the lowest energy transition at *ca.* 420 and 480 nm (Fig. 4).<sup>18</sup>

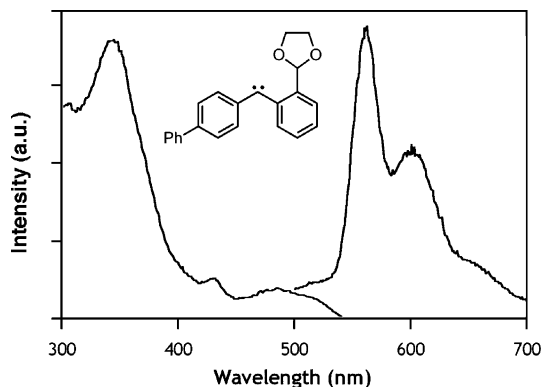
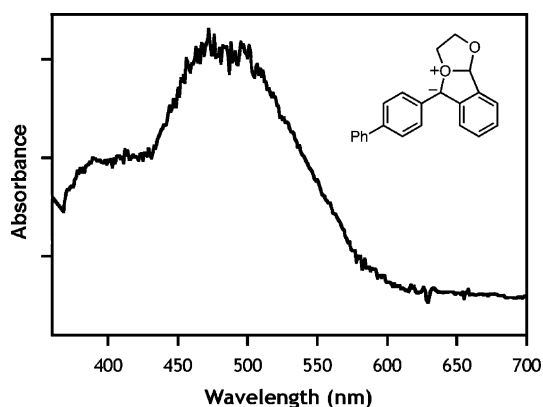


Fig. 4 Fluorescence excitation (left) and emission (right) spectra of  $^3C$ .

Irradiated samples of **1a** also showed a bright and persistent orange-red discoloration, suggesting the presence of a second non-fluorescent chromophore. A UV-Vis absorption revealed a very intense broad band with a  $\lambda_{\text{max}} = 490$  nm, which persists indefinitely at 77 K but disappears upon warming (Fig. 5). A control experiment with (4-phenyl)diphenyldiazomethane showed an indistinguishable carbene emission, but not the bright orange transient. Based on this observation we hypothesized that the



**Fig. 5** UV-Vis Absorption spectrum of the persistent signal assigned to ylide **Y**,  $\lambda_{\text{max}} \approx 490$  nm, which is formed by irradiation of diazo **1a** in MCH at 77 K.

490 nm transient corresponds to oxonium ylide **Y** (Schemes 2 and 4).

When microcrystalline samples of diazo **1a** were irradiated and analyzed at 77 K there was no detectable fluorescence of the triple carbene intermediate. Assuming that the carbene emission may be quenched by the diazo precursor we prepared mixed crystals with solutions containing 1% of diazo **1a** and 99% of ketoacetal **4**. It has been previously shown that analogous ketones and diazo compounds are able to form solid solutions,<sup>19</sup> a fact that can be easily confirmed by spectroscopic methods, including the visual reddish-orange coloration of the mixed crystals.

With time-dependent experiments carried out with excitation at  $\lambda = 350$  nm and front-face fluorescence detection at 550 nm we were able to detect the rapid growth of the carbene emission, which was followed by slower decay (Fig. 6). A full emission spectrum acquired with a fresh sample confirmed that the carbene was the emitting species. A qualitative correlation was observed between the decrease in the concentration of carbene  $^3\text{C}$  and an increase in the color of ylide **Y**. A time constant of *ca.* 200 s was estimated for the decay of the carbene signal, which did not go to zero, suggesting that an equilibrium was established. We also noticed that oxonium ylide **Y** is persistent for several hours at 77 K, both in glasses and in crystals, but it disappears rapidly upon warming.

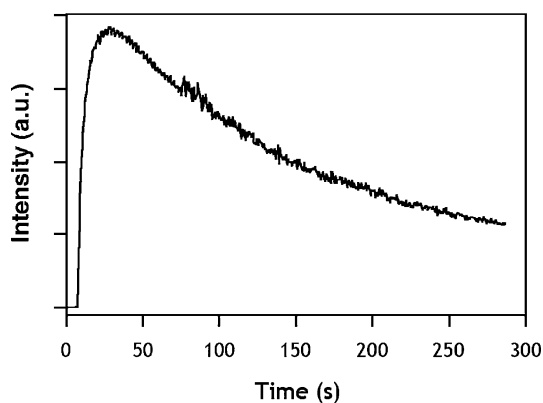


**Fig. 6** Emission growth and decay of carbene **C** in mixed crystals of **4** at 77 K.

## Reactions of carbenes and oxonium ylides

Our interpretation of the product analysis and spectroscopic data as a function of reaction media is based on the reaction pathways illustrated in Scheme 4. While it is well established that carbenes can be generated efficiently by photochemical excitation of diazo compounds both at ambient temperature and at 77 K,<sup>20</sup> the formation of oxonium ylides by reaction with ethers has been inferred mainly from product analysis studies.<sup>21</sup> The spectroscopic detection of oxonium ylides in solution by laser flash photolysis has been limited to a few carbenes with a singlet ground state.<sup>22,23</sup> A specific but reversible interaction between several free carbenes and ethers has been documented in terms of shifts in the carbene absorption spectrum<sup>24</sup> and/or in terms of extension of the carbene lifetime.<sup>14,25</sup> It is expected that the formation of oxonium ylides from aryl and diaryl carbenes will proceed through the thermally populated singlet state, such that triplet carbene, singlet carbene and oxonium ylide may coexist at concentrations that depend on their relative energies. Taking an experimentally determined Singlet–Triplet (S–T) gap of 2.6 kcal mol<sup>-1</sup> for diphenyl carbene as a guideline, we may estimate equilibrium populations at 300 K of the order of *ca.* 75 : 1 in favor of  $^3\text{C}$ .<sup>26</sup> While the relative energies of  $^1\text{C}$  and **Y** are not known at this time, a common feature of solution products **6**, **8** and **9** is that they all have the former diazo carbon attached to an oxygen atom, as expected for compounds that arise from an oxonium ylide intermediate. *ortho*-Quinodimethane **6** may be formulated as the result of a ring opening reaction and compounds **8** and **9** may be viewed as arising from two possible Stevens rearrangements. While the latter are described as formal 1,2-migrations of the anionic carbon to either of the two carbons flanking the oxonium center (illustrated by the blue and red arrows in the Scheme), based on evidence from analogous ammonium and sulfonium species it is commonly agreed that these reactions proceed by dissociative processes involving short-lived radical intermediates.<sup>27</sup> It is interesting that neither **7** nor **10**, which are the carbene-derived products, are detectable in benzene solution. This suggests that ylide formation and rearrangement from the singlet carbene must be favorable with respect to singlet C–H insertion. While it is likely that the triplet diaryl carbene is the most abundant species at equilibrium, it is well known that intramolecular hydrogen abstraction by triplet diaryl carbenes is a relatively slow process. In fact, *ortho*-methyl substituents have been used as “protecting” groups as they enhance the half-life of diphenylcarbene by factors of 10<sup>4</sup>–10<sup>5</sup>, into the ms regime.<sup>28,29</sup>

## Formation of carbenes and oxonium ylides

While the emission spectrum in Fig. 4 is identical to that obtained from samples of 4-phenyl-substituted diphenyldiazomethane, the spectrum in Fig. 5 was only observed for the compound bearing an *ortho*-acetal (**1a**). It is worth noting that the position of the absorption band is very similar to those previously reported for several types of oxonium ylides,<sup>14,23</sup> including those formed with 4-nitrophenylchlorocarbene,<sup>14,22a</sup> carbomethoxy-2-naphthylcarbene,<sup>22b</sup> and several alkyl-chlorocarbenes.<sup>23</sup> In fact, a recent computational and experimental study by Moss *et al.* on 4-nitrophenylchlorocarbene with several aliphatic and aromatic ethers reports a very appealing and elegant model regarding the spectroscopic characterization of “O-ylide”, “O-ylidic” and

" $\pi$ -complex" interactions.<sup>14</sup> The definitions proposed by Moss *et al.* are based on the formation of a "fully (or nearly fully) developed O–C bond", "an ether-carbene transient with O–C distances that exceed typical O–C bond lengths", and "charge transfer complexes formed between aromatic  $\pi$ -donors and carbene acceptors". With a combination of ground [PBE/6-311+G(d)] and excited state calculations [TD-B3LYP/6-311+G(d)//PBE/6-311+G(d)] to correlate the O–C bond distances with the absorption spectra, the authors proposed the following model: (1) O-ylides are characterized by O–C bonds of *ca.* 1.45 Å and an absorption band with a  $\lambda_{\text{max}}$  of 460–510 nm. O-Ylides were reported with 4-nitrophenylchlorocarbene with diethyl ether, THF and 18-crown-6. (2) O-Ylidic complexes, which can be observed with aromatic ethers such as anisole, 1,4-dimethoxybenzene and 1,2,3,5-tetramethoxybenzene, absorb in the same general region as the O-ylides, but (3) they are accompanied by the absorption of the  $\pi$ -complexes with a  $\lambda_{\text{max}}$  ~340–380 nm. Notably, as the O-ylidic species are less stable than the  $\pi$ -complexes, their relative absorbances display the changes in intensity expected for an equilibration process.

Based on the model suggested by Moss *et al.*,<sup>14</sup> the formation of a species with a  $\lambda_{\text{max}} \approx 480$  nm is consistent with an O-ylide or an O-ylidic interaction. The fact that the band appears to be indefinitely stable at 77 K is indicative of a species that exists in an energy well, but one can make no suggestions regarding its relative energy with respect to the undetected singlet state carbene. An X-ray-determined distance of 3.85 Å between the prospective carbene carbon and the closest oxygen atom in the crystals of **1a** (Ar<sub>2</sub>(N<sub>2</sub>)C–O) suggests that formation of ylide or ylidic complexes probably requires rotation of the dioxolane group with respect to the aromatic ring that bears the two groups. While it is likely that both oxonium ylide and carbene are present in the crystal, the only product observed at low (<20%) conversions is benzocyclobutane **10**, which probably originates from the triplet carbene precursor. The structure of **1a**, with a diazo carbon–acetal hydrogen C–H distance of 2.49 Å, should facilitate hydrogen abstraction by the triplet carbene followed by ring closure to generate **10** in a topochemically allowed reaction.<sup>30</sup> It is well known that reactions in crystals are determined by the size and shape of the reaction cavity rather than by the intrinsic energetics of the participant species.<sup>31</sup> While formation of the ylide intermediate may be within reach at early stages of the solid-to-solid conversion, it is likely that 1,2-migrations towards **8** and **9** may be sterically too demanding. The fact that these compounds are formed upon extended irradiation suggests that they form at defect sites.

## Conclusions

We have shown that suitably substituted carbene precursors may give rise to detectable, formally ionic oxonium ylide intermediates in non-polar organic glasses and in crystalline solids. Ruby-red crystals of diazo precursor **1a** were solved in the triclinic space group *P* $\bar{1}$ . The generation of oxonium ylide is supported by a strong UV absorption band with  $\lambda_{\text{max}} = 490$  nm at 77 K, and by rearrangement products in solution with a connectivity that derives from the expected O–C interaction, including *ortho*-quinodimethane **6**, dioxabicyclo[3.2.1]octane **8**, and 1,4-dioxane **9**. While detection of the ylide and the carbene suggest that reactions in crystals may occur under a pre-equilibrium, the

pristine solid at low conversion values favors the formation of a carbene-derived benzocyclobutane acetal. Since oxonium ylide products **8** and **9** are only detected at high conversion products they are likely to originate at defect sites. While a more detailed characterization of the reaction mechanism in solution and in crystals will require additional examples to establish the generality of this process, this study demonstrates that the scope of reactions in crystals may be much broader than is generally assumed.

## Experimental

<sup>1</sup>H and <sup>13</sup>C NMR spectra were obtained on an AMS 360 (360 MHz), Bruker ARX400 (400 MHz), or Avance Bruker ARX500 (500 MHz) spectrometer. <sup>1</sup>H and <sup>13</sup>C NMR spectra were obtained in C<sub>6</sub>D<sub>6</sub> or CDCl<sub>3</sub> with TMS as an internal standard, unless otherwise noted. IR spectra were obtained on a Perkin-Elmer Paragon 1000 FT-IR spectrometer. UV-Vis absorption spectra were acquired with a Hewlett-Packard 8453 spectrophotometer. Fluorescence spectra were recorded with a Spex-Fluorolog II spectrofluorimeter and corrected for nonlinear instrumental response. High-resolution electron impact (EI-HiRes) mass spectra were obtained on a VG Autospec (Micromass, Beverly, MA) spectrometer.

### 2-(2-Bromophenyl)-1,3-dioxolane **2**<sup>32</sup>

To a solution of 2-bromobenzaldehyde (8.0 g, 43.2 mmol) in 30 mL of benzene in a 50 mL three-necked round-bottomed flask were added in one portion anhydrous ethylene glycol (2.7 mL, 48 mmol) and *p*-toluenesulfonic acid monohydrate (5.29 mg, 27.8 mmol). The resulting solution mixture was refluxed until the theoretical yield of water had been collected in a Dean–Stark trap. TLC showed complete disappearance of the starting material. The mixture was cooled, washed with 10% aqueous sodium hydroxide (2 × 30 mL), followed by DI water (2 × 30 mL) and brine (1 × 30 mL), and the organic layer was dried over anhydrous MgSO<sub>4</sub>. The solvent was removed *in vacuo* and pumped under high vacuum to give 9.7 g (98%) of a clear yellow viscous oil;  $\nu_{\text{max}}/\text{cm}^{-1}$  (neat) 3067, 2954, 2888, 1593, 1571, 1473, 1443, 1388, 1270, 1211, 1125, 1092, 1042, 1023, 970, 944, 758.  $\delta_{\text{H}}$  (500 MHz, CDCl<sub>3</sub>) 7.59 (dd, *J* = 7.7, 1.8 Hz, 1H), 7.55 (dd, *J* = 8.0, 1.2 Hz, 1H), 7.32 (dt, *J* = 7.5, 1.2 Hz, 1H), 7.20 (dt, *J* = 7.9, 1.8 Hz, 1H), 6.09 (s, 1H), 4.16–4.09 (m, 2H), 4.07–4.01 (m, 2H);  $\delta_{\text{C}}$  (125 MHz, CDCl<sub>3</sub>) 136.50, 132.84, 130.50, 127.71, 127.30, 122.81, 102.47, 65.35; *m/z* (EI) 227.9788 (C<sub>9</sub>H<sub>9</sub>BrO<sub>2</sub> requires 227.9796).

### *o*-(1,3-Dioxolan-2-yl)phenyl(4-biphenyl)methanol **3**

Bromoacetal **2** (5.2 g, 22.70 mmol) was added to a 250 mL round-bottomed flask equipped with a magnetic stir bar. The flask was purged with argon for several minutes. Dry tetrahydrofuran (THF) was added to the acetal and then the solution was cooled to –78 °C in a dry ice–acetone bath. To the cooled solution at –78 °C, *n*-BuLi (15.6 mL, 1.6 M in hexanes) was added dropwise and then the reaction mixture was stirred for 1 h. A solution of 4-biphenylcarboxaldehyde (4.34 g, 23.82 mmol) in 50 mL of dry THF was then added slowly and the reaction mixture stirred overnight. Column chromatography of the crude reaction mixture on silica gel (4 : 1 hexanes–ethyl acetates, *v/v*) gave 6.6 g (88%) of a viscous yellow oil, which crystallized into a pale yellow solid over

two days;  $\nu_{\max}/\text{cm}^{-1}$  (neat) 3461 s (OH), 3029, 2974, 2889, 1599, 1449, 1409, 1387, 1351, 1221, 1108, 1072, 948, 768;  $\delta_{\text{H}}$  (500 MHz,  $(\text{CD}_3)_2\text{CO}$ ) 7.64–7.62 (m, 2H), 7.60–7.57 (m, 3H), 7.51–7.48 (m, 3H), 7.44–7.41 (m, 2H), 7.37–7.31 (m, 2H), 7.31–7.26 (m, 1H), 6.36 (d,  $J = 4.3$  Hz, 1H), 6.08 (s, 1H), 4.84 (d,  $J = 4.3$  Hz, 1H), 4.14–4.08 (m, 2H), 4.05–3.97 (m, 2H);  $\delta_{\text{C}}$  (125 MHz,  $(\text{CD}_3)_2\text{CO}$ ) 144.76, 144.61, 141.60, 140.19, 135.71, 129.79, 129.62, 128.66, 128.08, 127.98, 127.73, 127.59, 127.27, 126.91, 102.07, 70.83, 65.78, 65.77;  $m/z$  (EI) 332.1420 ( $\text{C}_{22}\text{H}_{20}\text{O}_3$  requires 332.1412).

#### ***o*-(1,3-Dioxolan-2-yl)phenyl(4-biphenyl)methanone 4**

Alcohol **3** (6.1 g, 18.35 mmol) was completely oxidized as reported by Swern<sup>33</sup> to yield 5.8 g (97%) of the ketone as a light pale yellow crystalline solid. TLC (3 : 1 hexane–ethyl acetates, v/v) showed complete oxidation of the starting alcohol and  $^1\text{H}$  and  $^{13}\text{C}$  NMR spectra in  $\text{CDCl}_3$  showed >95% purity. A portion of the crude ketone was purified by column chromatography on silica gel (3 : 1 hexanes–ethyl acetates, v/v). From the pure fractions after 1 day, large clear colorless plate-like needles grew. The colorless crystals were discovered to turn bright yellow upon exposure to 365 nm light (UV lamp) and reverted to the colorless state within less than one minute when the UV lamp was removed.  $\nu_{\max}/\text{cm}^{-1}$  (KBr) 3030, 2970, 2900, 1659 (C=O), 1604, 1580, 1484, 1447, 1402, 1307, 1280, 1266, 1214, 1113, 1066, 969, 932, 851, 794, 756, 702;  $\delta_{\text{H}}$  (500 MHz,  $\text{CDCl}_3$ ) 7.87 (d,  $J = 8.4$  Hz, 2H), 7.71 (d,  $J = 7.7$  Hz, 1H), 7.66 (d,  $J = 8.4$  Hz, 2H), 7.63–7.61 (m, 2H), 7.52 (dt,  $J = 7.7, 1.3$  Hz, 1H), 7.47–7.34 (m, 5H), 6.05 (s, 1H), 3.93–3.86 (m, 4H);  $\delta_{\text{C}}$  (125 MHz,  $\text{CDCl}_3$ ) 197.04 (C=O), 145.69, 139.80, 138.52, 136.80, 136.24, 130.60, 129.89, 128.88, 128.38, 128.17, 127.95, 127.22, 127.01, 126.94, 101.45, 65.10;  $m/z$  (EI) 330.1256 ( $\text{C}_{22}\text{H}_{18}\text{O}_3$  requires 330.1256).

#### ***o*-(1,3-Dioxolan-2-yl)phenyl(4-biphenyl)methanone hydrazone 5**

Ketone **4** (2.03 g, 6.14 mmol) and 50 mL of absolute ethanol were added to a three-necked round-bottomed flask equipped with a stir bar, Dean–Stark trap, and a water condenser. The suspension was heated to *ca.* 110 °C to dissolve all the ketone. To the refluxing reaction mixture, anhydrous hydrazine (7.5 mL, 0.239 mol) was added in one portion and the reaction was refluxed overnight (*ca.* 16 h), followed by an additional 24 h of refluxing. TLC (3 : 1 hexanes–ethyl acetate, v/v) showed four new spots, two above and two below the ketone. Excess ethanol and hydrazine were evaporated from the crude reaction in a rotary evaporator. The viscous organic layer was dissolved in 50 mL of diethyl ether, washed with DI water (3 × 50 mL), dried over anhydrous  $\text{MgSO}_4$ , filtered, and concentrated *in vacuo* to give a cloudy pale yellow viscous oil, which was purified by column chromatography on silica gel (3 : 1 hexanes–ethyl acetates, v/v) to yield 1.068 g (51%) of pure hydrazone as a pale yellow viscous oil.  $\nu_{\max}/\text{cm}^{-1}$  (KBr) 3404, 3290, 3029, 2888, 1576, 1487, 1397, 1331, 1270, 1211, 1114, 1070, 943, 846, 767, 731;  $\delta_{\text{H}}$  (500 MHz,  $\text{CDCl}_3$ ) 7.79–7.77 (m, 1H), 7.59–7.56 (m, 2H), 7.55–7.50 (m, 6H), 7.43–7.39 (m, 2H), 7.33–7.30 (m, 1H), 7.19–7.17 (m, 1H), 5.62 (s, 1H), 5.42 (br s, 2H, NH<sub>2</sub>), 4.14–4.00 (m, 2H), 3.93–3.87 (m, 2H);  $\delta_{\text{C}}$  (125 MHz,  $\text{CDCl}_3$ ) 147.71, 140.67, 140.62, 137.18, 136.41, 132.71, 130.63, 129.36, 128.99, 128.71, 127.47, 127.26, 126.91, 126.83, 126.38,

101.62, 65.51, 65.40;  $m/z$  (EI) 344.1523 ( $\text{C}_{22}\text{H}_{20}\text{N}_2\text{O}_2$  requires 344.1525).

#### ***o*-(1,3-Dioxolan-2-yl)phenyl(4-biphenyl)diazomethane 1a**

Hydrazone **5** (1 g, 2.90 mmol) was dissolved in 200 mL of anhydrous diethyl ether in a 500 mL round-bottomed flask equipped with a magnetic stir bar, to which anhydrous  $\text{MgSO}_4$  (2.58 g, 21.43 mmol) and yellow mercury(II) oxide (7 g, 32.32 mmol) were added to the stirring solution. A freshly prepared saturated solution of potassium hydroxide in absolute ethanol (20–30 drops) was added to initiate the oxidation of the hydrazone to the diazo compound. After the first 10 drops of the saturate KOH–EtOH solution, formation of a light pink color and darkening of the mercury(II)oxide were observed. NOTE: Addition of 1  $\mu\text{L}$  of anhydrous hydrazine to the reaction was sometimes necessary to initiate the oxidation. However, major darkening of the mercury(II) oxide was observed, to which an additional 2–3 spatula tips of fresh mercury(II) oxide were added. The reaction flask was wrapped with aluminium foil and stirred vigorously under an argon atmosphere at room temperature. After 8–10 hours of stirring under argon, complete consumption of the starting hydrazone was observed by TLC (2 : 1 hexanes–ethyl acetate, v/v). The reaction mixture was suction-filtered through a Hirsch funnel fitted with a glass microfibre (Whatman, 7.0 cm, 100 circles, Cat. No. 1820070) filter paper. The solution was concentrated by a flow of dry argon to give dark violet plates in near quantitative yields.  $\nu_{\max}/\text{cm}^{-1}$  (KBr) 3058, 3029, 2953, 2887, 2043, 1666, 1601, 1519, 1487, 1449, 1394, 1315, 1206, 1106, 1072, 972, 944, 833, 763;  $\delta_{\text{H}}$  (500 MHz,  $\text{CDCl}_3$ ) 7.78–7.74 (m, 1H), 7.58–7.53 (m, 4H), 7.48–7.47 (m, 3H), 7.43–7.40 (m, 2H), 7.33–7.29 (m, 1H), 6.98–6.96 (m, 2H), 5.88 (s, 1H), 4.13–4.08 (m, 2H), 4.00–3.95 (m, 2H);  $\delta_{\text{C}}$  (125 MHz,  $\text{CDCl}_3$ ) 140.55, 138.05, 136.72, 131.90, 130.79, 130.00, 129.23, 128.78, 128.74, 127.62, 127.60, 127.22, 127.03, 126.66, 122.60, 101.60, 65.49.

#### **General procedure and setup for photolysis in solution**

Approximately 10 mg of pure diazo was dissolved in *ca.* 1 mL of deuterated benzene. The solution was placed in an NMR tube and argon was slowly bubbled through the solution for 30 minutes to deoxygenate the sample. To the NMR tube, 1,1,2,2-tetrachloroethane (1 : 1 mole ratio of diazo to standard) was added to monitor the extent of conversion of starting material to products. Photolysis was carried out in a photolysis chamber (400 W mercury-vapor lamp) at room temperature with a 380 nm cutoff filter. The photolysis was monitored by  $^1\text{H}$  NMR every hour (total of *ca.* 6 h) until complete disappearance of the diazo was observed. The combined products were isolated by preparatory thin layer chromatography using a mixture of methylene chloride and hexanes (3 : 1 methylene chloride–hexanes, v/v).

#### **Solid-state photolysis**

Crystals of diazo **1a** (*ca.* 150 mg) were ground into a fine powder and placed into a Petri dish. A 380 nm cutoff filter was placed on top of the sample, which was placed over an aluminium block with an extension immersed in a large ice–water reservoir to help maintain the sample near 0 °C. The sample was exposed to UV light from a 400 W mercury vapor lamp kept in a jacket with circulating water kept at 0 °C. Reaction progress was monitored

by  $^1\text{H}$  NMR of samples taken at various intervals until complete disappearance of the starting material was observed.

#### (1*Z*,6*Z*)-1-(Biphenyl-4-yl)-3,4-dihydrobenzo[*f*] [1,4]dioxocine 9 (*o*-quinodimethane 6)

Isolated in 15% yield.  $\nu_{\text{max}}/\text{cm}^{-1}$  (neat) 3029, 2959, 2924, 2854, 1726 (w), 1629, 1598, 1521, 1488, 1405, 1345, 1280, 1262, 1067, 930, 844, 767;  $\delta_{\text{H}}$  (500 MHz,  $\text{C}_6\text{D}_6$ ) 7.81–7.79 (m, 2H), 7.44–7.42 (m, 4H), 7.22–7.19 (m, 3H), 6.73 (d,  $J = 9.3$  Hz, 1H), 6.16 (s, 1H), 5.88–5.85 (m, 1H), 5.83–5.80 (m, 1H), 5.66 (d,  $J = 9.1$  Hz, 1H), 3.77 (ddd,  $J = 8.6, 7.5, 1.0$  Hz, 1H), 3.69 (ddd,  $J = 11.6, 8.6, 5.4, 1\text{H}$ ), 2.07 (ddd,  $J = 12.3, 5.4, 1.0$  Hz, 1H), 1.44 (ddd,  $J = 12.3, 11.6, 7.5$  Hz, 1H);  $\delta_{\text{C}}$  (125 MHz,  $\text{CDCl}_3$ ) 150.24, 141.49, 140.38, 129.47, 128.84, 128.55, 127.60, 127.37, 127.04, 127.02, 123.41, 123.17, 120.92, 114.56, 112.73, 66.22, 39.08 (Note: one carbon could not be resolved);  $m/z$  (EI) : 314.1309 (314.1307 requires  $\text{C}_{22}\text{H}_{18}\text{O}_2$ ).

#### *cis*-1-(Biphenyl-4-yl)-benzo[*g*]2,5-dioxabicyclo[4.2.0]octane 9 (*cis*-1,4-dioxane 9)

Isolated in 43% yield.  $\nu_{\text{max}}/\text{cm}^{-1}$  (KBr) 3055, 3028, 2957, 2921, 2858, 1458, 1400, 1337, 1280, 1266, 1195, 1150, 1110, 1092, 1034, 823, 756;  $\delta_{\text{H}}$  (500 MHz,  $\text{CDCl}_3$ ) 7.59–7.57 (m, 4H), 7.49–7.40 (m, 7H), 7.37–7.32 (m, 2H), 5.34 (s, 1H), 4.05–3.99 (m, 1H), 3.90–3.80 (m, 3H);  $\delta_{\text{C}}$  (125 MHz,  $\text{CDCl}_3$ ) 147.09, 145.49, 140.75, 140.56, 140.39, 130.41, 130.03, 128.73, 127.28, 127.11, 127.08, 126.25, 124.41, 122.90, 83.26, 80.38, 61.66, 60.61;  $m/z$  (EI) 314.1309 ( $\text{C}_{22}\text{H}_{18}\text{O}_2$  requires 314.1307).

#### 5-(Biphenyl-4-yl)-benzo[*f*]2,8-dioxabicyclo[3.2.1]octane 8

Isolated in 15% yield.  $\nu_{\text{max}}/\text{cm}^{-1}$  (KBr) 3062, 3018, 2965, 2921, 2850, 1560, 1489, 1463, 1401, 1108, 1086, 966, 904, 749;  $\delta_{\text{H}}$  (500 MHz,  $\text{CDCl}_3$ ) 7.65–7.55 (m, 6H), 7.45–7.26 (m, 5H), 7.03 (d,  $J = 7.3$  Hz, 2H), 6.39 (s, 1H), 3.89 (ddd,  $J = 11.5, 12, 1.0$  Hz, 1H), 3.40 (ddd,  $J = 17, 12, 4$  Hz, 1H), 2.77 (ddd,  $J = 17, 13, 12$  Hz, 1H), 2.07 (ddd,  $J = 13, 4.0, 1.0$  Hz, 1H);  $\delta_{\text{C}}$  (125 MHz,  $\text{CDCl}_3$ ) 145.72, 140.95, 140.68, 139.62, 138.67, 128.91, 128.78, 128.13, 127.40, 127.20, 127.13, 125.88, 121.28, 120.19, 101.01, 85.74, 59.45, 35.70;  $m/z$  (tof) 314.1264 ( $\text{C}_{22}\text{H}_{18}\text{O}_2$  requires 314.1307).

#### 2-(Biphenyl-4-yl)-2*H*-spiro[cyclobutabenzene-1,2'-1,3]dioxolane] 10

Isolated in 75% yield.  $\delta_{\text{H}}$  (500 MHz,  $\text{CDCl}_3$ ) 7.59 (d,  $J = 7.3$  Hz, 2H), 7.55 (d,  $J = 8.1$  Hz, 2H), 7.48–7.30 (m, 7H), 7.24 (d,  $J = 8.2$  Hz, 2H), 4.97 (s, 1H), 4.19–4.11 (m, 2H), 4.03–3.99 (m, 1H), 3.70 (dd,  $J = 14.4, 7.0$  Hz, 1H);  $\delta_{\text{C}}$  (125 MHz,  $\text{CDCl}_3$ ) 145.36, 144.34, 140.95, 139.66, 137.55, 131.35, 128.84, 128.70, 128.57, 127.11, 127.02, 126.94, 123.69, 122.21, 111.25, 64.95, 64.68, 64.21;  $m/z$  (EI) 314.1337 ( $\text{C}_{22}\text{H}_{18}\text{O}_2$  requires 314.1307). The acetal was converted to the corresponding benzocyclobutenone by acid hydrolysis.  $\nu_{\text{max}}/\text{cm}^{-1}$  (neat) 1763 (s C=O), (*lit* C=O 1760  $\text{cm}^{-1}$ );<sup>16</sup>  $m/z$  (EI) 270.1039 ( $\text{C}_{20}\text{H}_{14}\text{O}$  requires 270.1045).

#### X-Ray diffraction

The X-ray intensity data were measured at 100 K on a Bruker SMART 1000 CCD-based X-ray diffractometer system equipped

with a Mo-target X-ray tube ( $\lambda = 0.71073$  Å) operated at 2250 W power. The detector was placed at a distance of 4.986 cm from the crystal. A total of 1321 frames were collected with a scan width of  $0.3^\circ$  in  $\omega$ , with an exposure time of 30 s/frame. The total data collection time was *ca.* 18 h. The frames were integrated with the Bruker SAINT software package using a narrow-frame integration algorithm. Analysis of the data showed negligible decay during the data collection. The structure was refined based on the respective space groups, using the Bruker SHELXTL (Version 5.3) Software Package.

**Compound 1a (X-ray).** Ruby-red plates were grown from diethyl ether, MW = 342.38, triclinic, space group  $P\bar{1}$ ,  $a = 6.0742(10)$  Å,  $b = 11.4003(18)$  Å,  $c = 12.3098(19)$  Å,  $\alpha = 93.982(3)^\circ$ ,  $\beta = 93.601(3)^\circ$ ,  $\gamma = 90.252(3)^\circ$ ,  $Z = 2$ ,  $\rho_{\text{calcd}} = 1.340$  mg  $\text{m}^{-3}$ ,  $F(000) = 360$ ,  $\lambda = 0.71073$  Å,  $\mu(\text{Mo K}\alpha) = 0.087$   $\text{mm}^{-1}$ ,  $T = 100(2)$  K, crystal size =  $0.4 \times 0.35 \times 0.2$   $\text{mm}^3$ . Of the 5564 reflections collected ( $1.66^\circ \leq \theta \leq 28.29^\circ$ ), 3874 [ $R(\text{int}) = 0.0138$ ] were independent reflections; max./min. residual electron density 311 and  $-201$   $e \text{ nm}^{-3}$ ,  $R1 = 0.0398$  [ $I > 2\sigma(I)$ ], and  $wR2 = 0.1185$  (all data).

**Compound 8 (X-ray).** Colorless plate-like needles grown from dichloromethane, MW = 314.36, monoclinic, space group  $P2_1/c$ ,  $a = 8.8692(18)$  Å,  $b = 7.5279(15)$  Å,  $c = 23.237(5)$  Å,  $\beta = 97.064(4)^\circ$ ,  $Z = 4$ ,  $\rho_{\text{calcd}} = 1.356$  mg  $\text{m}^{-3}$ ,  $F(000) = 664$ ,  $\lambda = 0.71073$  Å,  $\mu(\text{Mo K}\alpha) = 0.086$   $\text{mm}^{-1}$ ,  $T = 100(2)$  K, crystal size =  $0.3 \times 0.08 \times 0.05$   $\text{mm}^3$ . Of the 5448 reflections collected ( $1.77^\circ \leq \theta \leq 24.71^\circ$ ), 2207 [ $R(\text{int}) = 0.0575$ ] were independent reflections; max./min. residual electron density 177 and  $-192$   $e \text{ nm}^{-3}$ ,  $R1 = 0.0416$  [ $I > 2\sigma(I)$ ], and  $wR2 = 0.0795$  (all data).

#### Notes and references

- (a) *Reviews of Reactive Intermediates*, ed. M. S. Platz, R. A. Moss and M. Jones, John Wiley and Sons, Hoboken, NJ, 2007; (b) *Reactive Intermediate Chemistry*, ed. R. A. Moss, M. S. Platz and M. Jones, John Wiley and Sons, Hoboken, NJ, 2004.
- (a) T. Choi, K. Peterfy, S. I. Khan and M. A. Garcia-Garibay, *J. Am. Chem. Soc.*, 1996, **118**, 12477–12478; (b) K. Peterfy and M. A. Garcia-Garibay, *J. Am. Chem. Soc.*, 1998, **120**, 4540–4541; (c) Z. Yang and M. A. Garcia-Garibay, *Org. Lett.*, 2000, **2**, 1963–1965; (d) Z. Yang, D. Ng and M. A. Garcia-Garibay, *J. Org. Chem.*, 2001, **66**, 4468–4475; (e) D. Ng, Z. Yang and M. A. Garcia-Garibay, *Tetrahedron Lett.*, 2001, **42**, 9113–9116; (f) L. M. Campos, H. Dang, D. Ng, Z. Yang and M. A. Garcia-Garibay, *J. Org. Chem.*, 2002, **67**, 3749–3754; (g) D. Ng, Z. Yang and M. A. Garcia-Garibay, *Tetrahedron Lett.*, 2002, **43**, 7063–7066; (h) M. E. Ellison, D. Ng, H. Dang and M. A. Garcia-Garibay, *Org. Lett.*, 2003, **5**, 2531–2534.
- (a) S. H. Shin, A. E. Keating and M. A. Garcia-Garibay, *J. Am. Chem. Soc.*, 1996, **118**, 7626–7627; (b) S. H. Shin, D. Cizmeciyan, A. E. Keating, S. I. Khan and M. A. Garcia-Garibay, *J. Am. Chem. Soc.*, 1997, **119**, 1859–1868; (c) C. N. Sanrame, C. P. Suhrada, H. Dang and M. A. Garcia-Garibay, *J. Phys. Chem. A*, 2003, **107**, 3287–3294.
- M. A. Garcia-Garibay, *Acc. Chem. Res.*, 2003, **36**, 491–498.
- (a) M. A. Garcia-Garibay, A. E. Constable, J. Jernelius, T. Choi, D. Cizmeciyan and S. H. Shin, *Physical Supramolecular Chemistry*, Kluwer Academic Publishers, Dordrecht, 1996; (b) A. E. Keating, M. A. Garcia-Garibay, in *Molecular and Supramolecular Photochemistry*, ed. V. Ramamurthy and K. Schanze, Marcel Dekker, New York, 1998, vol. 2, pp. 195–248.
- (a) S. H. Shin, A. E. Keating and M. A. Garcia-Garibay, *J. Am. Chem. Soc.*, 1996, **118**, 7626–7627; (b) S. H. Shin, D. Cizmeciyan, A. E. Keating, S. I. Khan and M. A. Garcia-Garibay, *J. Am. Chem. Soc.*, 1997, **119**, 1859–1868.
- M. A. Garcia-Garibay, S. Shin and C. N. Sanrame, *Tetrahedron*, 2000, **56**, 6729–6737.



- 8 (a) H. Tomioka, N. Hayashi, Y. Izawa, V. P. Senthilnathan and M. S. Platz, *J. Am. Chem. Soc.*, 1983, **105**, 5053–5057; (b) M. A. Garcia-Garibay, *J. Am. Chem. Soc.*, 1993, **115**, 7011–7012; (c) M. A. Garcia-Garibay, C. Theroff, S. H. Shin and J. Jernelius, *Tetrahedron Lett.*, 1993, **52**, 8415–8418.
- 9 L. M. Campos and M. A. Garcia-Garibay, *Reactive Intermediates in Crystals: Form and Function*, in *Reviews of Reactive Intermediate Chemistry*, ed. M. S. Platz, M. Jones, R. Moss, Wiley-Interscience, Hoboken, NJ, 2007.
- 10 (a) A. Padwa and S. F. Hornbuckle, *Chem. Rev.*, 1991, **91**, 263–309; (b) J. S. Clark, *Nitrogen, Oxygen and Sulfur Ylide Chemistry: A Practical Approach in Chemistry*, Oxford University Press, Oxford, 2002.
- 11 (a) Oxonium ylides and synthesis: X. Guo, H. Huang, L. Yang and W. Hu, *Org. Lett.*, 2007, **9**, 4721–4723; (b) G. K. Murphy, F. P. Marmsaeter and F. G. West, *Can. J. Chem.*, 2006, **84**; (c) J. M. Mejia-Oneto and A. Padwa, *Org. Lett.*, 2006, **8**, 3275–3278; (d) F. P. Marmsaeter, G. K. Murphy and F. G. West, *J. Am. Chem. Soc.*, 2003, **126**, 14724–14725; (e) A. Oku, N. Murai and J. Baird, *J. Org. Chem.*, 1997, **62**, 2123–2129.
- 12 W. Kirmse and K. Kund, *J. Am. Chem. Soc.*, 1989, **111**, 1465–1473.
- 13 (a) K. B. Eisenthal, N. J. Turro, E. V. Sitzmann, I. R. Gould, G. Hefferon, J. Langan and Y. Cha, *Tetrahedron*, 1985, **41**, 1543; (b) D. Griller, A. S. Nazran and J. C. Scaiano, *Tetrahedron*, 1985, **41**, 1525.
- 14 R. A. Moss, L. Wang, E. Weintraub and K. Krogh-Jespersen, *J. Am. Chem. Soc.*, 2008, **130**, 4651–4659.
- 15 (a) E. Migirdicyan and J. Baudet, *J. Am. Chem. Soc.*, 1975, **97**, 7400–7404; (b) C. R. Flynn and J. Michl, *J. Am. Chem. Soc.*, 1974, **96**, 3280–3288.
- 16 (a) R. V. Stevens and G. S. Bisacchi, *J. Org. Chem.*, 1982, **47**, 2396–2399; (b) R. V. Stevens and G. S. Bisacchi, *J. Org. Chem.*, 1982, **47**, 2393–2396.
- 17 (a) A. M. Trozzolo and W. A. Gibbons, *J. Am. Chem. Soc.*, 1967, **89**, 239–243; (b) J. C. Scaiano, *Solution Photochemistry of Carbenes and Biradicals*, ed. M. S. Platz, Plenum Press, New York, 1990, pp. 353–368.
- 18 J. C. Scaiano and D. Weir, *Can. J. Chem.*, 1988, **66**, 491–494.
- 19 (a) R. W. Brandon, G. L. Closs, C. E. Davoust, C. A. Hutchison, Jr., B. E. Kohler and R. Silbey, *J. Chem. Phys.*, 1965, **43**, 2006; (b) C. Cheng, T. -S. Lin and D. J. Sloop, *Chem. Phys. Lett.*, 1976, **44**, 576; (c) D. C. Doetschman and C. A. Hutchison, *J. Chem. Phys.*, 1972, **56**, 3964; (d) D. J. Graham and T. -S. Lin, *Chem. Phys. Lett.*, 1982, **73**, 411; (e) A. M. Trozzolo, E. Wasserman and W. A. Yager, *J. Chim. Phys.*, 1964, **61**, 1663; (f) R. J. M. Anderson, B. E. Kohler and J. M. Stevenson, *J. Chem. Phys.*, 1979, **71**, 1559; (g) H. Sixl, R. Mathes, A. Schaupp and K. Ulrich, *Chem. Phys.*, 1986, **107**, 105.
- 20 M. S. Platz, in *The Chemistry, Kinetics, and Mechanisms of Triplet Carbene Processes in Low Temperature Glasses and Solids*, ed. M. S. Platz, Plenum Press, New York, 1990, pp. 143–212.
- 21 (a) Product analysis: M. Jones, Jr. and R. T. Ruck, *Tetrahedron Lett.*, 1998, **39**, 2277–2280; (b) T. Sueda, T. Nagaoka, S. Goto and M. Ochiai, *J. Am. Chem. Soc.*, 1996, **118**, 10141–10149; (c) H. Tomioka, N. Kobayashi, S. Murata and Y. Ohtawa, *J. Am. Chem. Soc.*, 1991, **113**, 8771–8778.
- 22 (a) S. Celebi, M. -L. Tsao and M. S. Platz, *J. Phys. Chem. A*, 2001, **105**, 1158–1162; (b) J. -L. Wang, T. Yuzawa, M. Nigam, I. Likhovorik and M. S. Platz, *J. Phys. Chem. A*, 2001, **105**, 3752–3756; (c) E. M. Tippman, M. S. Platz, I. B. Svir and O. V. Klymenko, *J. Am. Chem. Soc.*, 2004, **126**, 5750–5762.
- 23 R. A. Moss, J. Tiang, R. R. Sauers and K. Krogh-Jespersen, *J. Am. Chem. Soc.*, 2007, **129**, 10019–10028.
- 24 I. Naito, A. Oku, N. Otani, Y. Fujiwara and Y. Tanimoto, *J. Chem. Soc., Perkin Trans. 2*, 1996, 725–729.
- 25 R. A. Moss, J. Tian, R. R. Sauers and K. Krogh-Jespersen, *J. Am. Chem. Soc.*, 2007, **129**, 10019.
- 26 K. B. Eisenthal, R. A. Moss and N. J. Turro, *Science*, 1984, **225**, 1439–1445.
- 27 (a) W. D. Ollis, M. Rey, I. O. Sutherland and G. L. Closs, *J. Chem. Soc., Chem. Commun.*, 1975, 543; (b) H. Iwamura, M. Iwamura, T. Nishida, M. Yoshida and J. Nakayama, *Tetrahedron Lett.*, 1971, 63.
- 28 W. Kirmse, *Angew. Chem., Int. Ed.*, 2003, **42**, 2117–2119.
- 29 (a) H. Tomioka, H. Okada, T. Watanabe and K. Hirai, *Angew. Chem., Int. Ed. Engl.*, 1994, **33**, 873–875; (b) H. Tomioka, H. Okada, T. Watanabe, K. Banno, K. Komatsu and K. Hirai, *J. Am. Chem. Soc.*, 1997, **119**, 1582–1593; (c) Y. -M. Hu, K. Hirai and H. Tomioka, *J. Phys. Chem. A*, 1999, **103**, 9280–9284; (d) K. Hirai, K. Yasuda and H. Tomioka, *Chem. Lett.*, 2000, 94–95; (e) Y. -M. Hu, Y. Ishikawa, K. Hirai and H. Tomioka, *Bull. Chem. Soc. Jpn.*, 2001, **74**, 2207–2218; (f) K. Hirai, T. Iikubo and H. Tomioka, *Chem. Lett.*, 2002, 1226–1227; (g) T. Iikubo, K. Hirai and H. Tomioka, *Org. Lett.*, 2002, **4**, 2261–2264; (h) T. Koshiyama, K. Hirai and H. Tomioka, *J. Phys. Chem. A*, 2002, **106**, 10261–10274.
- 30 (a) G. M. J. Schmidt, *Solid State Photochemistry*, Verlag Chemie, New York, 1976; (b) G. J. M. Schmidt, *Pure Appl. Chem.*, 1971, **27**, 647.
- 31 M. D. Cohen, *Angew. Chem., Int. Ed. Engl.*, 1975, **14**, 386.
- 32 (a) G. D. Hartman, B. T. Phillips and W. Halczenko, *J. Org. Chem.*, 1985, **50**, 2423–2427; (b) G. D. Hartman, W. Halczenko and B. T. Phillips, *J. Org. Chem.*, 1985, **50**, 2427–2431.
- 33 (a) A. J. Mancuso and D. Swern, *Synthesis*, 1981, 165–185; (b) A. J. Mancuso, D. S. Brownfain and D. Swern, *J. Org. Chem.*, 1979, **44**, 4148–4150; (c) A. J. Mancuso, S. -L. Huang and D. Swern, *J. Org. Chem.*, 1978, **43**, 2480–2482.